Experimental Studies of Light-Induced Charge Transfer and Charge Redistribution in (X 2 - Bipyridine)Re I (CO) 3 Cl Complexes

ARTICLE *in* INORGANIC CHEMISTRY · JULY 2002

Impact Factor: 4.76 · DOI: 10.1021/ic011015g · Source: PubMed

3 AUTHORS, INCLUDING:

Keith A. Walters
Northern Kentucky University
28 PUBLICATIONS **610** CITATIONS
SEE PROFILE

Joseph Hupp
Northwestern University
519 PUBLICATIONS **28,908** CITATIONS
SEE PROFILE

Inorg. Chem. **2002**, *41*, 2909–2919

Experimental Studies of Light-Induced Charge Transfer and Charge Redistribution in (X_2-Bipyridine)$Re^{I}(CO)_3Cl$ Complexes

Keith A. Walters, Young-Jin Kim, and Joseph T. Hupp*

Department of Chemistry, Northwestern University, 2145 Sheridan Road, Evanston, Illinois 60208-3113

Received September 28, 2001

Stark emission spectroscopy, transient DC photoconductivity (TDCP), and ground-state dipole moment measurements have been used to evaluate charge transfer (CT) within various (X_2-bipyridine)$Re^{I}(CO)_3Cl$ complexes following ^{3}MLCT excited-state formation. The Stark technique reports on vector differences between ground-state (μ_g) and excited-state (μ_e) dipole moments, while TDCP, when combined with independently obtained μ_g information, reports on scalar differences. For systems featuring collinear, same-signed ground- and excited-state dipole moments, the scalar and vector differences are equivalent. However, for the low symmetry systems studied here, they are distinctly different. The vector difference yields the effective adiabatic one-electron-transfer distance (R_{12}), while the combined vector and scalar data yield information about dipole rotation upon ground-state/excited-state interconversion. For the systems examined, charge transfer distances are substantially smaller than geometric electron-donor/electron-acceptor site separation distances. The measured distances are significantly affected by changes in acceptor ligand substituent composition. Electron-donating substituents decrease CT distances, while electron-withdrawing substituents increase CT distances, as do aromatic substituents that are capable of expanding the bipyridyl ligand (acceptor ligand) π system. The Stark measurements additionally indicate that the CT vector and the transition dipole moment are significantly orthogonal, a consequence of strong polarization of the Re–Cl bond (orthogonal to the metal/acceptor-ligand plane) in the ground electronic state and relaxation of the polarization in the upper state. The ground-state Re–Cl bond polarization is sufficiently large that the overall ground-state scalar dipole moment exceeds the overall excited-state scalar dipole moment, despite transfer of an electron from the metal center to the diimine ligand. This finding provides an explanation for the otherwise puzzling negative solvatochromism exhibited in this family of compounds. Combining TDCP and Stark results, we find that the dipole moment can be rotated in some instances by more than 90° upon ^{3}MLCT excited-state formation. The degree of rotation or reorientation can be modulated by changing the identity of the acceptor ligand substituents. Reorientational effects are smallest when the compounds feature aromatic substituents capable of spatially extending the π system of the acceptor ligand.

Introduction

Long-lived, photochemically generated excited states of second- and third-row transition metal complexes usually feature significant triplet character and often are based on internal charge transfer, for example, metal-to-ligand charge transfer (MLCT).[1] From a fundamental perspective, a key element of any molecular charge-transfer process is the adiabatic CT distance, R_{12}.[2−5] From a functional perspective, the CT distance can report on upper-state charge delocalization (for example, within extended aromatic electron-acceptor ligands). It can also determine, in large measure, the degree to which solvent and other environmental factors couple to an electronic transition. We[6−8] and many others[3,9−14] have taken advantage of electroabsorption spectroscopy (Stark spectroscopy) to determine CT distances in inorganic

* Corresponding author. E-mail: jthupp@chem.nwu.edu. Fax: (847) 491-7713.

(1) (a) Newton, M. D. *Chem. Rev.* **1991**, *91*, 761−792. (b) Barbara, P. F.; Meyer, T. J.; Ratner, M. A. *J. Phys. Chem.* **1996**, *100*, 13148−13168.

(2) (a) Oh, D. H.; Boxer, S. G. *J. Am. Chem. Soc.* **1990**, *112*, 8161−8162. (b) Oh, D. H.; Sano, M.; Boxer, S. G. *J. Am. Chem. Soc.* **1991**, *113*, 6880−6890.

(3) Shin, Y. K.; Brunschwig, B. S.; Creutz, C.; Sutin, N. *J. Am. Chem. Soc.* **1995**, *117*, 8668−8669.

(4) Reimers, J. R.; Hush, N. S. *J. Phys. Chem.* **1991**, *95*, 9773−9781.

(5) Cave, R.; Newton, M. D. *Chem. Phys. Lett.* **1996**, *249*, 15−19.

10.1021/ic011015g CCC: $22.00
Published on Web 04/19/2002

systems. Briefly, the second-derivative component of an electroabsorption spectrum yields the excited-state/ground-state dipole moment difference (vector difference), $|\Delta\mu_v|$, which in turns equals $e \cdot R_{12}$, where e is the unit electronic charge.

While the electroabsorption technique is indeed powerful, there are circumstances where it is inapplicable. For example, the desired electronic transition may be obscured by other more intense transitions, or the excited state of interest may be a dark state. A case in point is the prototypical inorganic chromophore (bpy)$Re^{I}(CO)_3Cl$ (bpy is 2,2′-bipyridine).[15−18] The compound emits from an MLCT excited state (eq 1) that is nominally triplet in character, making direct excitation to this state effectively spin-forbidden.

$$(bpy^{\bullet -})Re^{II}(CO)_3Cl \rightarrow (bpy)Re^{I}(CO)_3Cl + h\upsilon_{em} \quad (1)$$

The corresponding ^{1}MLCT transition is allowed and does feature significant extinction. However, it overlaps strongly with higher energy bipyridine-localized $^1\pi-\pi^*$ transitions, severely complicating electroabsorption investigations. We reasoned that CT distance information could more effectively be obtained by instead examining the reverse process, emission from the ^{3}MLCT excited state, via electric-field-effect spectroscopy (Stark emission spectroscopy),[19] and by additionally employing a conceptually different approach: transient direct current photoconductivity (TDCP).[20,21]

Scheme 1

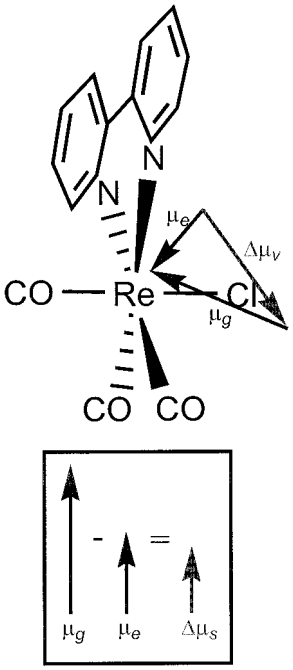

We have previously reported in a preliminary fashion on the TDCP behavior of (bpy)$Re^{I}(CO)_3Cl$ (**1**).[8] Like Stark spectroscopy, TDCP reports on excited-state/ground-state dipole moment differences. The quantities obtained, however, are the *scalar*, rather than *vector*, dipole moment differences (Scheme 1). TDCP further differs from Stark spectroscopy in that it also yields the sign of the dipole moment difference. A particularly striking outcome from the preliminary study of **1** was the observation that the scalar dipole moment of the "charge separated" excited state was substantially *smaller* than the dipole moment of the ground state.[8] This finding, while clearly unusual, provided an explanation for some otherwise puzzling behavior patterns for **1**, including negative solvatochromism.[15,17,18]

As described further in this work, by combining these two techniques, one can move beyond simple CT distance assessment and begin to examine light-induced charge *redistribution*. We present here the results of combined Stark emission and TDCP studies of an extended family of (bpy)-$Re^{I}(CO)_3Cl$ type complexes (**1**−**7**, Scheme 2) featuring a range of chemically modified bipyridine ligands (electron-accepting, -donating, or -delocalizing ligands). We were particularly interested in understanding how expanding the ligand π system would affect CT distances and charge redistribution. We were similarly interested in understanding whether and how ligand substituent properties would modulate CT distances and redistribution behavior. We find that both kinds of perturbations are significant. More generally, the new study offers insight into the phenomenon of and consequences of photoexcitation of low symmetry charge-transfer systems.

Experimental Section

Materials and Characterization. All reagents and materials were used as received from Aldrich or Fluka. Tetrahydrofuran (THF) was distilled from sodium metal/benzophenone. Triethyl-

(6) Karki, L.; Hupp, J. T. *Inorg. Chem.* **1997**, *36*, 3318−3321.
(7) (a) Karki, L.; Vance, F. W.; Hupp, J. T.; LeCours, S. M.; Therien, M. J. *J. Am. Chem. Soc.* **1998**, *120*, 2606−2611. (b) Karki, L.; Williams, R. D.; Hupp, J. T.; Allen, C. B.; Spreer, L. O. *Inorg. Chem.* **1998**, *37*, 2837−2840. (c) Vance, F. W.; Hupp, J. T. *J. Am. Chem. Soc.* **1999**, *121*, 4047−4053.
(8) Vanhelmont, F. W. M.; Hupp, J. T. *Inorg. Chem.* **2000**, *39*, 1817−1819.
(9) For a recent review on Stark-effect spectroscopy, see: Bublitz, G. U.; Boxer, S. G. *Annu. Rev. Phys. Chem.* **1997**, *48*, 213−242.
(10) For a review of Stark-effect spectroscopy of metal complexes, see: Vance, F. W.; Williams, R. D.; Hupp, J. T. *Int. Rev. Phys. Chem.* **1998**, *17*, 307−329.
(11) (a) Locknar, S. A.; Peteanu, L. A. *J. Phys. Chem. B* **1998**, *102*, 4240−4246. (b) Chowdury, A. C.; Locknar, S. A.; Premvardhan, L. L.; Peteanu, L. A. *J. Phys. Chem. A* **1999**, *103*, 9614−9625. (c) Premvardhan, L. L.; Peteanu, L. A. *J. Phys. Chem. A* **1999**, *103*, 7506−7514.
(12) Walters, K. A.; Premvardhan, L. L.; Liu, Y.; Peteanu, L. A.; Schanze, K. S. *Chem. Phys. Lett.* **2001**, *339*, 255−262.
(13) Shin, Y. K.; Brunschwig, B. S.; Creutz, C.; Sutin, N. *J. Phys. Chem.* **1996**, *100*, 8157−8169.
(14) Brunschwig, B. S.; Creutz, C.; Sutin, N. *Coord. Chem. Rev.* **1998**, *177*, 61−79.
(15) Wrighton, M.; Morse, D. L. *J. Am. Chem. Soc.* **1974**, *96*, 998−1003.
(16) Wrighton, M. S.; Morse, D. L.; Pdungsap, L. *J. Am. Chem. Soc.* **1975**, *97*, 2073−2079.
(17) Giordano, P. J.; Wrighton, M. S. *J. Am. Chem. Soc.* **1979**, *101*, 2888−2897.
(18) Worl, L. A.; Duesing, R.; Chen, P.; Della Ciana, L.; Meyer, T. J. *J. Chem. Soc., Dalton Trans.* **1991**, 849−858.
(19) (a) Lockhart, D. J.; Hammes, S. L.; Franzen, S.; Boxer, S. G. *J. Phys. Chem.* **1991**, *95*, 2217−2226. (b) Baumann, W.; Bischof, H. *J. Mol. Struct.* **1985**, *129*, 125−136. (c) Baumann, W.; Spohr, E.; Bischof, H.; Liptay, W. *J. Lumin.* **1987**, *37*, 227−233. (d) Lockhart, D. J.; Boxer, S. G. *Chem. Phys. Lett.* **1988**, *144*, 243−250. (e) Lockhart, D. J.; Goldstein, R. F.; Boxer, S. G. *J. Chem. Phys.* **1988**, *89*, 1408−1415.
(20) Smirnov, S. N.; Braun, C. L. *J. Phys. Chem.* **1994**, *98*, 1953−1961.
(21) Smirnov, S. N.; Braun, C. L. *Rev. Sci. Instrum.* **1998**, *69*, 2875−2887.

Scheme 2

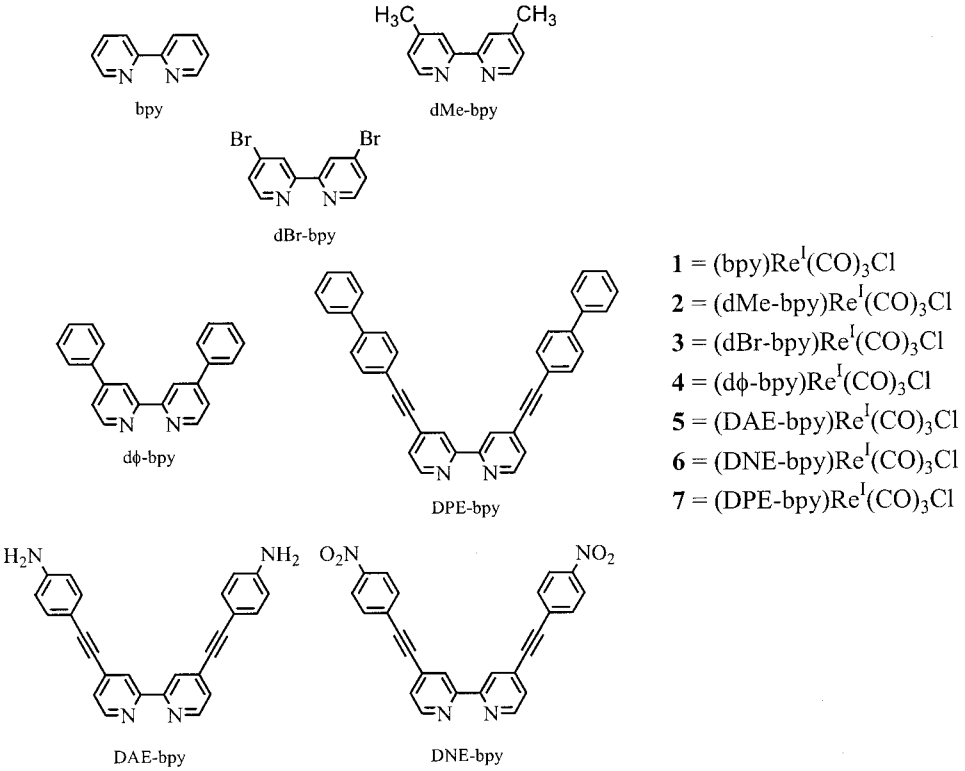

amine and toluene were distilled prior to use. $Re(CO)_5Cl$ was purchased from Aldrich. The ligands 2,2′-bipyridine (bpy), 4,4′-dimethyl-2,2′-bipyridine (dMe-bpy), and 4,4′-diphenyl-2,2′-bipyridine (dϕ-bpy) were also purchased from Aldrich, along with the substituted aryl halides 4-bromobiphenyl, 1-bromo-4-nitrobenzene, and 4-iodoaniline. 4,4′-Dibromo-2,2′-bipyridine (dBr-bpy) was prepared according to previously published procedures,[22] along with the rhenium complexes (bpy)Re(CO)$_3$Cl (**1**), (dMe-bpy)Re(CO)$_3$Cl (**2**), (dBr-bpy)Re(CO)$_3$Cl (**3**), and (dϕ-bpy)Re(CO)$_3$Cl (**4**).[18] All syntheses were performed under argon unless otherwise noted. ^{1}H and ^{13}C NMR spectra were recorded on a Varian Mercury-400 MHz spectrometer. Mass spectrometry (MS) measurements used standard FAB conditions for ligands and metal complexes. All spectra agreed with appropriate simulations. Elemental analyses were performed by ORS, Oneida, NY.

Synthesis. *para*-Substituted Ethynylbenzene Compounds. These compounds were prepared by modification of previously published procedures.[23] To a mixture of trimethylsilylacetylene (2.36 g, 24 mmol) and substituted aryl halide (20 mmol) in dry triethylamine (80 mL) bis(Triphenylphosphine)palladium dichloride (0.28 g, 0.4 mmol) and copper(I) iodide (0.02 g, 0.2 mmol) were added. The reaction mixture was stirred at room temperature for 6 h under nitrogen followed by solvent evaporation. The residue was dissolved in ethanol, aqueous potassium hydroxide (10 mL, 1.0 M) was added, and the mixture was stirred at room temperature for 2 h. After solvent removal, the residue was extracted with chloroform and washed with water. The chloroform was finally removed by rotary evaporation. The crude products were recrystallized from ethanol.

***para*-phenylethynylbenzene.** Substituted aryl halide: 4-bromobiphenyl. Yield: 1.89 g (53%). ^{1}H NMR ($CDCl_3$): δ = 3.14 (s, 1H), 7.39 (d, 2H, J = 7.2 Hz), 7.47 (d, 2H, J = 8.4 Hz), 7.58 (m, 5H) ppm. MS (FAB): m/z = 178 [M$^+$].

***para*-nitroethynylbenzene.** Substituted aryl halide: 1-bromo-4-nitrobenzene. Yield: 2.3 g (78%). ^{1}H NMR ($CDCl_3$): δ = 3.37 (s, 1H), 7.65 (d, 2H, J = 12.0 Hz), 8.21 (d, 2H, J = 12.0 Hz) ppm. MS (FAB): m/z = 147 [M$^+$].

***para*-aminoethynylbenzene.** Substituted aryl halide: 4-iodoaniline. Yield: 1.2 g (51%). ^{1}H NMR ($CDCl_3$): δ = 2.97 (s, 1H), 6.61 (d, 2H, J = 11.2 Hz), 7.31 (d, 2H, J = 11.6 Hz) ppm. MS (FAB): m/z = 117 [M$^+$].

4,4′-diarylethynyl-2,2′-bipyridine Compounds. A solution of 4,4′-dibromo-2,2′-bipyridine (1.2 g, 3.82 mmol), a *para*-substituted-ethynylbenzene (8.0 mmol), bis(triphenylphosphine)palladium dichloride (0.28 g, 0.4 mmol), copper(I) iodide (0.02 g, 0.2 mmol), and triethylamine (15 mL) in dry THF (40 mL), was refluxed for 16 h. After this period, the reaction mixture was cooled and the solvent removed by rotary evaporation. The residue was dissolved in methylene chloride and washed with water. The organic extract was dried over anhydrous sodium sulfate, and the solvent was removed by rotary evaporation. The crude product was purified by flash column chromatography (silica gel, eluent CH_2Cl_2/hexanes/MeOH 6:3:1) and recrystallized from warm ethanol to yield the final product.

4,4′-di(phenylethynylbenzene)-2,2′-bipyridine (DPE-bpy). Yield: 0.95 g (49%). ^{1}H NMR ($CDCl_3$): δ = 7.54 (d, 4H, J = 4.8 Hz), 7.65 (d, 4H, J = 4.8 Hz), 8.55 (d, 2H, J = 5.6 Hz), 8.68 (s, 6H), 8.93 (d, 2H, J = 5.6 Hz), 9.18 (d, 2H, J = 4.8 Hz) ppm. Anal. Calcd for $C_{38}H_{24}N_2$: C, 89.12; H, 4.69; N, 5.47. Found: C, 89.15; H, 4.51; N, 5.42. MS (FAB): m/z = 510 [M$^+$].

4,4′-di(nitroethynylbenzene)-2,2′-bipyridine (DNE-bpy). Yield: 0.97 g (57%). ^{1}H NMR ($CDCl_3$): δ = 7.47 (s, 2H), 7.58 (d, 4H, J = 8.4 Hz), 7.67 (d, 2H, J = 8.0 Hz), 7.74 (d, 2H, J = 8.0 Hz), 8.28 (d, 2H, J = 8.4 Hz) ppm. Anal. Calcd for $C_{26}H_{14}N_4O_4$: C, 69.97; H, 3.14; N, 12.56. Found: C, 69.82; H, 3.07; N, 12.52. MS (FAB): m/z = 445 [M$^+$].

(22) Maerker, G.; Case, F. C. *J. Am. Chem. Soc.* **1958**, *80*, 2745−2748.
(23) (a) Allen, A. D.; Cook, C. D. *Can. J. Chem.* **1963**, *41*, 1084−1087. (b) Lavastre, O.; Ollivier, L.; Dixneuf, P. H.; Sibandhit, S. *Tetrahedron* **1996**, *52*, 5495−5504.

4,4′-di(aminoethynylbenzene)-2,2′-bipyridine (DAE-bpy). Yield: 2.5 g (32%). ^{1}H NMR ($CDCl_3$): $\delta = 6.68$ (d, 4H, $J = 8.4$ Hz), 7.43 (d, 4H, $J = 8.4$ Hz), 7.68 (d, 2H, $J = 5.0$ Hz), 8.33 (s, 2H), 8.92 (d, 2H, $J = 5.6$ Hz) ppm. Anal. Calcd for $C_{26}H_{28}N_4$: C, 78.79; H, 7.09; N, 14.14. Found: C, 78.62; H, 7.16; N, 14.11. MS (FAB): $m/z = 387$ [M^+].

***fac*-(4,4′-X$_2$-2,2′-bipyridine)Re(CO)$_3$Cl Complexes.** (4,4′-X$_2$-bipyridine)Re(CO)$_3$Cl complexes were synthesized via a general procedure modified from ref 18. A solution of $Re(CO)_5Cl$ (0.103 g, 0.285 mmol) and the bipyridine ligand (0.285 mmol) in 20 mL of dry toluene was refluxed for 1.5 h. After the mixture cooled to room temperature,[24] the (diimine)Re(CO)$_3$Cl precipitated, and the yellow or orange product was collected by filtration on a sintered glass filter and dried.

(DAE-bpy)Re(CO)$_3$Cl (5). Yield: 0.16 g (87%). ^{1}H NMR (CD_3COCD_3): $\delta = 6.73$ (d, 4H, $J = 7.6$ Hz), 7.37 (d, 4H, $J = 8.4$ Hz), 7.72 (d, 2H, $J = 5.2$ Hz), 8.00 (s, 2H), 8.96 (d, 2H, $J = 5.2$ Hz) ppm. ^{13}C NMR (CD_3COCD_3): $\delta = 179, 172, 157, 154, 150, 134, 132, 129, 115, 108, 83, 72, 48$ ppm. Anal. Calcd for $C_{29}H_{18}N_4O_3ClRe$: C, 50.33; H, 2.60; N, 8.10. Found: C, 49.86; H, 2.84; N, 8.03. MS (FAB): $m/z = 693.4$ [M^+], 658 [$M^+ - Cl$].

(DNE-bpy)Re(CO)$_3$Cl (6). Yield: 0.12 g (84%). ^{1}H NMR (DMSO-d_6): $\delta = 7.03$ (d, 4H, $J = 8.0$ Hz), 7.09 (d, 2H, $J = 5.2$ Hz), 7.43 (d, 4H, $J = 8.0$ Hz), 8.20 (d, 2H, $J = 12.0$ Hz), 8.28 (s, 2H) ppm. ^{13}C NMR (DMSO-d_6): $\delta = 186, 175, 140, 136, 133, 128, 125, 124, 117, 87, 60, 48, 41$ ppm. Anal. Calcd for $C_{29}H_{14}N_4O_7ClRe$: C, 46.32; H, 1.86; N, 7.45. Found: C, 46.11; H, 1.98; N, 7.36. MS (FAB): $m/z = 752.7$ [M^+], 717.1 [$M^+ - Cl$].

(DPE-bpy)Re(CO)$_3$Cl (7). Yield: 0.18 g (79%). ^{1}H NMR (DMSO-d_6): $\delta = 6.19$ (d, 4H, $J = 5.0$ Hz), 6.28 (d, 4H, $J = 5.0$ Hz), 6.83 (d, 2H, $J = 8.0$ Hz), 7.06 (s, 6H), 7.88 (s, 2H), 8.25 (d, 2H, $J = 8.0$ Hz) ppm. ^{13}C NMR (DMSO-d_6): $\delta = 174, 171, 164, 163, 156, 152, 150, 147, 143, 142, 140, 136, 134, 133, 129, 127, 125, 123, 116, 108$ ppm. Anal. Calcd for $C_{41}H_{24}N_2O_3ClRe$: C, 60.5; H, 2.95; N, 3.44. Found: C, 59.7; H, 2.43; N, 3.12. MS (FAB): $m/z = 815.1$ [M^+], 779.2 [$M^+ - Cl$].

Conventional Photophysical Measurements. UV−vis spectra were measured for CH_2Cl_2 solutions with a HP 8452A diode array spectrophotometer. IR data (KBr pellets) were collected on a Biorad FTIR spectrophotometer. Steady-state fluorescence spectra were obtained using an ISA Fluorolog Model FL3-11 spectrophotometer. Luminescence lifetime data were obtained with a Photon Technologies International Timemaster stroboscopic detection instrument with a gated nitrogen lamp (337 nm excitation) using a scatter solution to profile the instrument response function. Lifetimes were deconvoluted using an iterative reconvolution procedure. The luminescence lifetime of (DAE-bpy)Re$^{\rm I}$(CO)$_3$Cl was separately obtained using a previously described setup.[25] Transient absorption lifetimes (where specified) were obtained using 355 nm excitation and a setup profiled earlier.[26] Single exponential decays were obtained in all cases.

Stark Emission Measurements. Stark emission measurements were conducted on poly(methyl methacrylate) (PMMA) thin films of the rhenium complexes. The films were prepared by dissolving the analyte complex in a dichloroethylene solution containing PMMA (Aldrich, $M_w \approx 996$ kD, 0.75 g/15 mL), filtering the solution through a 0.22 μm Teflon filter, and drop casting a film in an aluminum dish that was dried overnight. Film thicknesses were determined by measuring the spacing of interference peaks in IR spectra of the films and were typically 180−200 μm.[6] Prior to measurement, a 2 × 2 cm square of the film was pressed between two ITO-coated pieces of glass with spring clips and heated in a drying oven (∼50 °C) for 20 min to evaporate any residual dichloroethylene and ensure a good electrical contact. Samples were placed in a home-built liquid nitrogen immersion dewar, and an electric field was generated with a Joseph Rolfe Associates Model 1100 AC power supply (typical fields were 2×10^7 V m^{-1}). Samples were excited at their MLCT absorption maximum. Emitted light was measured through a horizontal polarizer in the Fluorolog spectrophotometer using front-face acquisition geometry. The emission spectrum and change-in-emission spectrum were simultaneously recorded on a Stanford Research Systems SR 850 digital lock-in amplifier at twice the AC field modulation frequency (200 Hz). Spectra were recorded at angles (χ) of 90° and 62.5° between the light propagation vector and electric field.[27]

Analysis of the data obtained is done in a fashion closely analogous to Stark absorption[6] and is only briefly summarized here. The Stark emission data are fit to a linear combination of the zeroth, first, and second derivatives of the luminescence spectrum $F(\upsilon)$:

$$\frac{2\sqrt{2}\Delta F(\upsilon)}{F_{\max}} = \left\{A_\chi F(\upsilon) + \frac{B_\chi}{15hc}\frac{\upsilon^3 \mathrm{d}[F(\upsilon)/\upsilon^3]}{\mathrm{d}\upsilon} + \frac{C_\chi}{30h^2c^2}\frac{\upsilon^3 \mathrm{d}^2[F(\upsilon)/\upsilon^3]}{\mathrm{d}\upsilon^2}\right\}\mathbf{E}_{\rm int}{}^2 \quad (2)$$

In eq 2, $\Delta F(\upsilon)$ is the frequency-dependent emission change resulting from the electric field modulation, $F_{\max}$ is the intensity maximum of $F(\upsilon)$, h is Planck's constant, c is the speed of light in a vacuum, υ is the frequency of the emitted light, and $\mathbf{E}_{\rm int}$ is the internal electric field experienced by the chromophore.[28] The coefficients A_χ, B_χ, and C_χ provide information about the changes in the transition dipole, polarizability, and dipole moment, respectively, and are described as follows:

$$A_\chi = \frac{\langle \boldsymbol{\alpha}_{\mathbf{m}} \rangle}{3} + {}^1/_{30}(3\cos^2\chi - 1)[3\langle \boldsymbol{\beta}_{\mathbf{m}} \rangle - 2\langle \boldsymbol{\alpha}_{\mathbf{m}} \rangle] \quad (3)$$

$$B_\chi = {}^5/_2 \mathrm{Tr}\Delta\alpha + (3\cos^2\chi - 1)({}^3/_2 \hat{\mathbf{g}}\cdot\Delta\alpha\cdot\hat{\mathbf{g}} - {}^1/_2 \mathrm{Tr}\,\Delta\alpha) \quad (4)$$

$$C_\chi = |\Delta\mu_{\rm v}|^2[5 + (3\cos^2\xi - 1)(3\cos^2\chi - 1)] \quad (5)$$

In these equations, $\langle \boldsymbol{\alpha}_{\mathbf{m}} \rangle$ and $\langle \boldsymbol{\beta}_{\mathbf{m}} \rangle$ are the scalar portions of the transition moment polarizability and hyperpolarizability tensors, $\mathrm{Tr}\Delta\alpha$ is the trace of the polarizability change between the ground and excited electronic states, $\hat{\mathbf{g}}\cdot\Delta\alpha\cdot\hat{\mathbf{g}}$ is the polarizability change along the transition moment ($\hat{\mathbf{g}}$ is the unit vector), $\Delta\mu_{\rm v}$ is the vector change in dipole moment, and ξ is the angle between the transition dipole moment and $\Delta\mu_{\rm v}$ vector.[6] Three film samples were prepared and measured for each complex, and the resulting calculated parameters were averaged.

TDCP Measurements. All measurements were performed with the same instrumentation as described earlier,[8,25] with the exception that a flow cell was used (∼8 mL min^{-1} flow rate) to minimize sample photodegredation and reduce the potential for irreversible electrochemistry to degrade the sample. A 1000 V potential was

(24) In the case of (DNE-bpy)Re(CO)$_3$Cl, the reaction mixture was filtered hot to remove any unreacted ligand. The product was subsequently precipitated by slowly adding hexanes.

(25) Vanhelmont, F. W. M.; Johnson, R. C.; Hupp, J. T. *Inorg. Chem.* **2000**, *39*, 1814−1816.

(26) (a) Greenfield, S. R.; Svec, W. A.; Gosztola, D.; Wasielewski, M. R. *J. Am. Chem. Soc.* **1996**, *118*, 6767−6777. (b) Gaal, D. A.; Hupp, J. T. *J. Am. Chem. Soc.* **2000**, *122*, 10956−10963.

(27) The second angle takes into account the refraction of the incident radiation through the ITO cell; see ref 11b.

(28) $\mathbf{E}_{\rm int} = f\cdot\mathbf{E}_{\rm external}$; f(PMMA) has been estimated as 1.11 by: Ponder, M.; Mathies, R. *J. Phys. Chem.* **1983**, *87*, 5090−5098.

applied over the 0.46 mm electrode gap during the experiments. All complexes were studied in saturated solutions of 1:1 chloroform/toluene that were prepared by dissolving the samples in chloroform, filtering through a 0.22 μm Teflon filter, and diluting the filtrates dropwise with equal quantities of toluene. All solutions were argon bubble deoxygenated for 30 min prior to study and excited with the 355 nm third harmonic of a Quantel Brilliant Nd:YAG laser (10 Hz, 4 ns fwhm). Laser energies of ~150−250 μJ pulse^{-1} were typically used to irradiate the samples. Solution optical densities were between 0.5 and 1.0 at the excitation wavelength.

The methodology of TDCP data analysis has been reported previously,[8,25] but the basic ideas are summarized here. The mathematical theory of TDCP stems from the polarization of a single analyte system in the probed solution, P_{solute}:[29]

$$P_{solute} = n_i \frac{\mu_i^2 E_c}{3k_b T} \tag{6}$$

In eq 6, n_i is the solute dipole concentration, μ_i is the solute dipole moment, E_c is the internal electric field, k_b is Boltzmann's constant, and T is temperature. If the temporal evolution of P_{solute} concomitant with photoexcitation is considered, one obtains

$$\Delta P_{solute}(t) = n_e(t)(\mu_e^2 - \mu_g^2)\frac{E_c}{3k_b T} \tag{7}$$

In this equation, $n_e(t)$ is the time-dependent excited-state dipole population. Note that the dipole moment difference is reflected as a *difference of squares*, thus requiring independent determination of μ_g to calculate charge transfer distances. The evolving transient current, $v(t)$, can be related to $\Delta P_{solute}(t)$ by the following expression:

$$v(t) + \tau_{RC}\frac{dv(t)}{dt} = \frac{\varphi R V_0 \mu_e^2 - \mu_g^2 dn_e}{d \quad 3k_b T \quad dt} \tag{8}$$

In eq 8, τ_{RC} is the circuit RC time constant, φ is a solvent-dependent correction parameter that varies between 1.3 and 1.9,[20,30] d is the distance between electrodes in the TDCP cell, R is the resistance that the measured voltage is taken across (50 Ω), and V_0 is the applied DC voltage. Five measurements were recorded on each sample solution, deconvoluted on the basis of eq 8 to obtain the so-called "effective" scalar dipole moment change ($\Delta\mu_{s,eff} = \sqrt{|\mu_e^2 - \mu_g^2|}$), and averaged to obtain the reported value.

Ground-State Dipole Measurements. Ground-state dipole moments were obtained from solution conductivity measurements via eq 9:[31]

$$\left(\frac{\epsilon - 1}{\epsilon + 2}\right) - \left(\frac{\eta^2 - 1}{\eta^2 + 2}\right) = \frac{4\pi N_A \mu_g^2 C}{9k_b T \epsilon_0} \tag{9}$$

where ϵ is the sample solution dielectric constant, η is the sample solution refractive index,[32] N_A is 6.02 × 10^{23} molecules mol^{-1}, μ_g is the analyte molecule ground-state dipole moment in esu·cm (1 D = 1 × 10^{-18} esu·cm), C is the analyte concentration in the sample solution (mole mL^{-1}), k_b is Boltzmann's constant (1.38066 × 10^{-16} erg K^{-1}), and $\epsilon_0 = 1/4\pi$. Dielectric constant measurements were conducted with a Dielectric Products Company (Watertown, MA) Model 350G three-electrode liquid dielectric cell[33] and a GenRad GR1658 Digibridge digital impedance meter. Conductivity and dispersion values of 1:1 chloroform/toluene solutions of the complexes[34] were determined using eqs 10 and 11[35] with a 1 kHz test frequency and averaged over 10 data acquisition cycles.

$$\epsilon = \frac{C_p}{C_0} \tag{10}$$

$$C_p = \frac{C_x}{1 + D^2} \tag{11}$$

In the equations, C_0 is the measured air capacitance of the cell (33 pF), C_x is the measured sample solution capacitance, and D is the measured sample solution dispersion (typically ≈ 0). At least three sample concentrations in the concentration range 2−5 × 10^{-4} M were measured for each complex, producing a linear plot based on eq 9 that was used to extract $\mu_{g,exp}$.

Calculations. A geometry optimization was performed on each of the rhenium complexes using the PC SPARTAN Plus software package. The final molecular coordinates from the optimization were used for a single point ZINDO-1 CI calculation in Hyperchem 5.11. Parameters for manganese and chlorine were used as needed in place of rhenium and bromine, respectively, because semiempirical parameters were not available for these atoms.

Table 1. (X$_2$-bpy)Re^I(CO)$_3$Cl Photophysical Characterization[a]

	X	λ_{max}/nm (ϵ_{max}/10^3 M^{-1} cm^{-1})	λ_{em}/nm (τ_{em}/ns)	υ(C≡O)/cm^{-1}
1	H	388 (2.1)	598 (39[b])	2023, 1917, 1900[b]
2	CH_3	378 (3.4)	589 (49[b])	2022, 1915, 1897[b]
3	Br	408 (2.7)	657 (8)	2019, 1935, 1871
4	ϕ	396 (9.9)	610 (56[b])	2019, 1918, 1875[b]
5	DAE	408 (18)	628 (54)	2021, 1911, 1894
6	DNE	422 (8.4)	653 (70[c])	2021, 1916, 1897
7	DPE	410 (7.1)	640 (12[c])	2020, 1935, 1872

[a] All measurements are at room temperature in CH_2Cl_2 except for υ(C≡O), which is in KBr. Errors for τ_{em} are ±10%. [b] Reference 18. [c] Lifetime determined by transient absorption measurements.

Results

Synthesis and Photophysical Characterization. A series of (X$_2$-bpy)Re(CO)$_3$Cl complexes **1**−**7** (Scheme 2) was synthesized and characterized. Complexes **1**, **2**, and **4** were previously investigated by Meyer and co-workers, and our photophysical results duplicate their observations.[18,36] Spectral characterization data, including IR peaks in the C≡O stretch region, UV−vis absorption maxima, and luminescence maxima and lifetimes, are listed in Table 1. All absorption spectra show intense UV absorptions due to

(29) Debeye, P. *Polar Molecules*; Dover: New York, 1929.
(30) Smirnov, S. N.; Braun, C. L.; Greenfield, S. R.; Svec, W. A.; Wasielewski, M. R. *J. Phys. Chem.* **1996**, *100*, 12329−12336.
(31) (a) Janini, G. M.; Katrib, A. H. *J. Chem. Educ.* **1983**, *60*, 1087−1088. (b) Chen, C. T.; Liao, S. Y.; Lin, K. J.; Chen, C. H.; Lin, T. Y. J. *Inorg. Chem.* **1999**, *38*, 2734−2741. (c) Kott, K. L.; Whitaker, C. M.; McMahon, R. J. *Chem. Mater.* **1995**, *7*, 426−439.
(32) In eq 6, the refractive index of the solvent without analyte is typically used as η since the value does not significantly change after analyte addition.
(33) (a) D 150-87: Standard Test Methods for A-C Loss Characteristics and Permittivity (Dielectric Constant) of Solid Electrical Insulating Materials. American Society for Testing and Materials, 1987. (b) D 924-92: Standard Test Method for Dissipation Factor (or Power Factor) and Relative Permittivity (Dielectric Constant) of Electrical Insulating Liquids. American Society for Testing and Materials, 1992.
(34) Ground-state dipole moment measurements on complexes **2**, **4**, and **7** were performed in chloroform solutions because of the limited solubilities of these complexes in 1:1 chloroform/toluene.
(35) Breitung, E. M.; Vaughan, W. E.; McMahon, R. J. *Rev. Sci. Instrum.* **2000**, *71*, 224−227.
(36) Caspar, J. V.; Meyer, T. J. *J. Phys. Chem.* **1983**, *87*, 952−957.

bipyridine-centered $^1\pi-\pi^*$ transitions. In each case, a separate band or shoulder at lower energy (the reported maximum) is observed that is strongly solvatochromic. Consistent with the behavior of other (diimine)$Re^I(CO)_3Cl$ and $Re^I(CO)_3Cl(pyridine)_2$ complexes,[15,17,18] negative solvatochromic effects are observed (i.e., absorption bands shift to higher energy with increasing solvent polarity). These observations lead to the assignment of the shoulders as rhenium-to-bipyridine charge-transfer transitions. Three strong stretches are observed in the C≡O stretch region in each of the IR spectra, consistent with a facial orientation of the carbonyl ligands.[18]

Before proceeding further, a brief comment on the electron-donating, -withdrawing, and/or -delocalizing nature of each substituted bipyridine is in order. For the "simple" bipyridines, the order of increasing electron-withdrawing ability is **2** < **1** < **3**. Relative to **1**, the phenyl-substituted bipyridine complex (**4**) exhibits both electron-withdrawing and -delocalizing effects. The addition of ethynyl spacers is anticipated to amplify both of these effects. Complex **6** is clearly more strongly withdrawing than **5**, but the strength of **5** relative to **4** is not clear. The available IR data for **7**, especially for the middle-frequency CO ligand, suggest that the substituents for this compound are strongly electron withdrawing.[18]

The solution-phase MLCT absorption is highest in energy when X is an electron-donating group (378 nm for **2**) and lowest when X is an electron-withdrawing group (408 nm for **3**). The same trend is observed in the emission band maxima (589 and 657 nm, respectively, for the two complexes). The maxima are blue-shifted by ~20 nm in the rigid low-temperature PMMA environment (see Table 1). The spectra offer no evidence of chromophore aggregation.[37] Like the excited-state emission energies, excited-state lifetimes (τ, Table 1), acquired at room temperature in solution, also display a sensitivity to ligand substituent composition.

Substitution of aryl groups on the bipyridine ligand decreases the MLCT absorption (e.g., 396 nm for **4** compared to 388 nm for **1**) and emission (610 and 598 nm, respectively) energies. These variations likely reflect opposing effects: (1) an energy decrease (wavelength increase) due to increased intraligand electron delocalization in the aryl-containing MLCT excited state and (2) a smaller energy decrease due to the electron-withdrawing nature of the aryl substituents (note, in particular, compound **7**). The presence of electron-donating and -withdrawing groups in **5** and **6**, respectively, further contributes to their photophysical characteristics via combinations of the trends described previously.

Stark Emission Measurements. Even at reduced temperatures, (X_2-bpy)$Re^I(CO)_3Cl$ ^{3}MLCT phosphorescence is weak, resulting in comparatively noisy Stark emission spectra. Consequently, only the portion of the spectrum immediately around the phosphorescence band was employed in data fits. A representative Stark emission study for **1** is shown in Figure 1. The top panel shows the normalized emission spectrum, and its second derivative is shown in the middle panel. The Stark emission signals for two values of χ are shown in the bottom panel. Note the similar band shapes in the second and third panels, implying a significant C_χ term, and consequently $|\Delta\mu_v|$, contribution to the Stark spectrum (eq 5). Further illustration of the contributions of each derivative component of eq 2 is shown in Figure 2, again indicating a significant second derivative component. The values for $|\Delta\mu_v|$, $Tr\Delta\alpha$, $\hat{\mathbf{g}}\cdot\Delta\alpha\cdot\hat{\mathbf{g}}$, and ξ resulting from fits to eqs 2−5 are listed in Table 2.

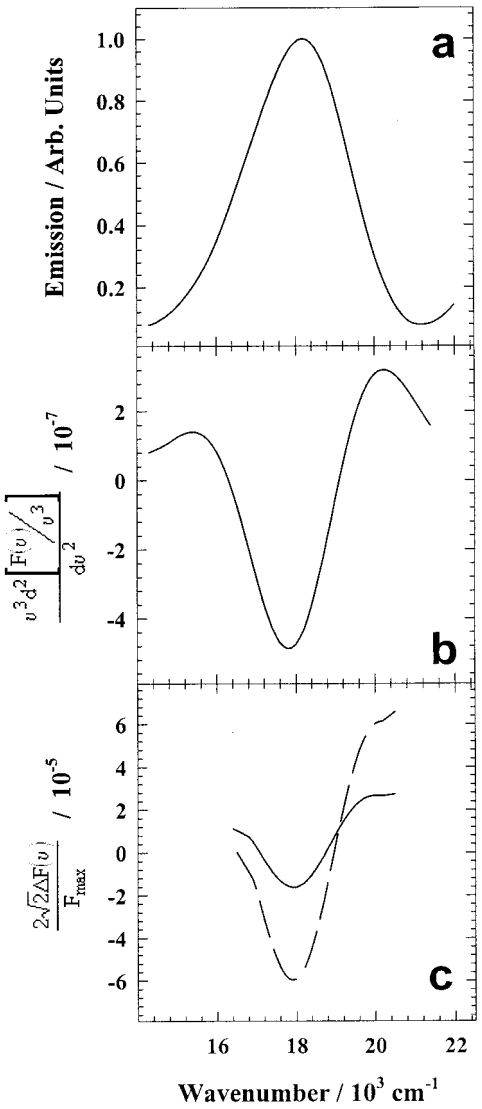

Figure 1. Stark emission data of **1** in a PMMA thin film (182.1 μm thick) at 77 K. (a) Normalized emission spectrum. (b) Second derivative of emission spectrum. (c) Stark emission signal at $\chi = 90°$ (solid line, × 2) and $\chi = 62.5°$ (dashed line).

For the series of compounds, a few trends are clearly evident. Electron-donating substituents on either the simple bipyridine ligand (**2**) or the phenyl-ethynyl bipyridine ligand (**5**) decrease $|\Delta\mu_v|$, while electron-withdrawing substituents (**3** and **6**) increase its value. The addition of phenyl rings alone (**4**) does not result in a dramatic change in $|\Delta\mu_v|$, but further expansion of the diimine ligand in **7** does yield an increase. The polarizability data exhibit a more complex

(37) Walters, K. A.; Ley, K. D.; Schanze, K. S. *Langmuir* **1999**, *15*, 5676−5680.

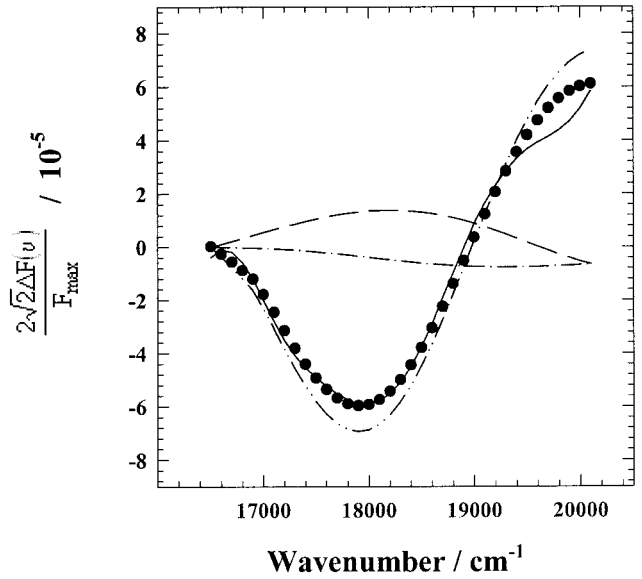

Figure 2. Stark emission deconvolution components of **1** in a PMMA thin film (182.1 μm thick, $\chi = 62.5°$) at 77 K. The solid line is experimental data, and the deconvolution fit is shown as circles. The contributions of the zeroth, first, and second derivatives to the fit (eq 2) are indicated by the dashed, dot−dashed, and dot−dot−dashed lines, respectively.

Table 2. (X$_2$-bpy)Re^I(CO)$_3$Cl Stark Emission Data[a]

	X	$\lvert\Delta\mu_v\rvert$[b]/D (e Å)	Tr$\Delta\alpha$[c]/Å^3	$\hat{\mathbf{g}}\cdot\Delta\alpha\cdot\hat{\mathbf{g}}$[d]/Å^3	ξ[e]/°
1	H	9 (1.9)	22	27	90
2	CH_3	7.4 (1.6)	460	880	90
3	Br	12 (2.6)	300	240	90
4	ϕ	9.5 (2.0)	400	430	50
5	DAE	9 (1.9)	−220	−1400	47
6	DNE	14 (3.0)	−140	−840	49
7	DPE	12 (2.5)	−290	−690	43

[a] All measurements performed on PMMA thin films (∼180 μm thickness) at 77 K. Uncertainties in $\lvert\Delta\mu_v\rvert$ varied between ±8 and 11% (standard deviations from measurements with multiple samples). [b] Vector dipole moment difference. [c] Trace of the polarizability change. [d] Polarizability change along the transition moment. [e] Angle between the transition dipole moment and the $\Delta\mu_v$ vector.

pattern. Positive values for both polarizability parameters are found for complexes **1**−**4**, but negative values are found for **5**−**7**.

One parameter that returned unusual results was ξ, the angle between the transition dipole, which in this molecule runs from the rhenium center towards the bipyridine ligand, and the $\Delta\mu$ vector. For complexes **1**−**3** (i.e., those with ligands lacking electron-delocalizing substituents), ξ was 90°, suggesting approximate orthogonality between these vectors. However, complexes featuring electron-delocalizing substituents (**4**−**7**) were characterized by significantly smaller ξ values.

TDCP and Ground-State Dipole Moment Measurements. The desire to understand in greater detail the relative geometries of ground- and excited-state dipole moments prompted the application of the TDCP technique. Representative TDCP signals are shown in Figure 3 for complex **3**. Consistent with our earlier studies of **1**,[8,38] all TDCP signals

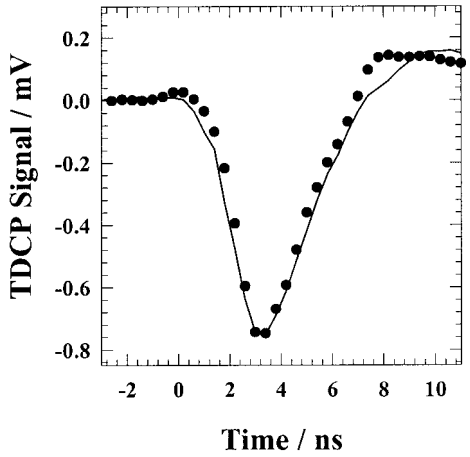

Figure 3. Representative TDCP signal (lines) and fit based on eq 8 (dots) of complex **3**. Data from 1:1 chloroform/toluene solution.

Table 3. (X$_2$-bpy)Re^I(CO)$_3$Cl TDCP Data[a]

	X	$\Delta\mu_{s,eff}$[b]/D	$\mu_{g,calcd}$[c]/D	$\mu_{g,exp}$[d]/D	μ_e[g]/D	$\Delta\mu_s$[h]/D	$\lvert\Delta\mu_v\rvert$[i]/D	$\theta_{\Delta\mu}$[j]/°
1	bpy	−7.0	12	7.7	3.0	−4.7	9.0	110
2	Me	−8.8	13	9.7[e]	4.0	−5.6	7.4	64
3	Br	−7.8	12	9.0	4.7	−4.4	12	120
4	ϕ	−8.0	13	11[e]	7.7	−3.3	9.5	60
5	DAE	−7.5	14	(15)[f]	13	−2.0	9.0	40
6	DNE	−4.5	13	(12)[f]	11	−0.9	14	75
7	DPE	−8.3	13	9.0[e]	3.7	−5.4	12	130
8	Mn(bpy)		12	6.9				

[a] All measurements performed in 1:1 chloroform/toluene unless otherwise noted. [b] Effective scalar dipole moment difference (see footnote 39). [c] Ground-state dipole moment determined by semiempirical calculations. [d] Ground-state dipole moment determined by dielectric constant measurements. [e] Chloroform solution. [f] $\mu_{g,exp}$ value extrapolated from the linear relationship of $\mu_{g,exp}$ to $\mu_{g,calcd}$, see text. [g] Excited-state dipole moment. [h] Scalar dipole moment difference. [i] Vector dipole moment difference. [j] Angle between μ_g and μ_e.

were negative at short and intermediate times after the laser pulse, indicating smaller values for $\lvert\mu_e\rvert$ than $\lvert\mu_g\rvert$. Fits of the TDCP signals using eq 8[8,21] yielded values for $\mu_e^2 - \mu_g^2$. The square root of this quantity, $\Delta\mu_{s,eff}$, is listed in Table 3.[39]

Estimation of scalar dipole moment changes, $\Delta\mu_s = \mu_e - \mu_g$, from the TDCP response requires values for μ_g. These values were determined experimentally ($\mu_{g,exp}$) via dielectric constant measurements on solutions with varying complex concentrations (eqs 9−11). Values for six of the eight rhenium complexes and one manganese analogue are listed in Table 3. Notably, the ground-state dipole moment is measurably smaller for (bpy)Mn^I(CO)$_3$Cl than (bpy)Re^I(CO)$_3$Cl.

Unfortunately, because of poor solubility in the low polarity solvents required for ground-state dipole moment measurements, values for **5** and **6** could not be obtained via dielectric constant measurements. Consequently, we resorted to computational estimates (semiempirical electronic structure calculations). Because parameters were unavailable for

(38) In ref 8, we reported a $\Delta\mu_{s,eff}$ of ∼9 D. This value is higher than the current value, likely because of slight sample degradation during the earlier TDCP experiment, an effect that has been mitigated here by employing a flow cell.

(39) Note that $\mu_e^2 - \mu_g^2$ is negative for all complexes studied here. The square root of this difference would be an imaginary number, so the absolute value of this difference is used to determine $\Delta\mu_{s,eff}$. The negative sign is assigned to this value to illustrate the negative difference in the squares of the dipole moments.

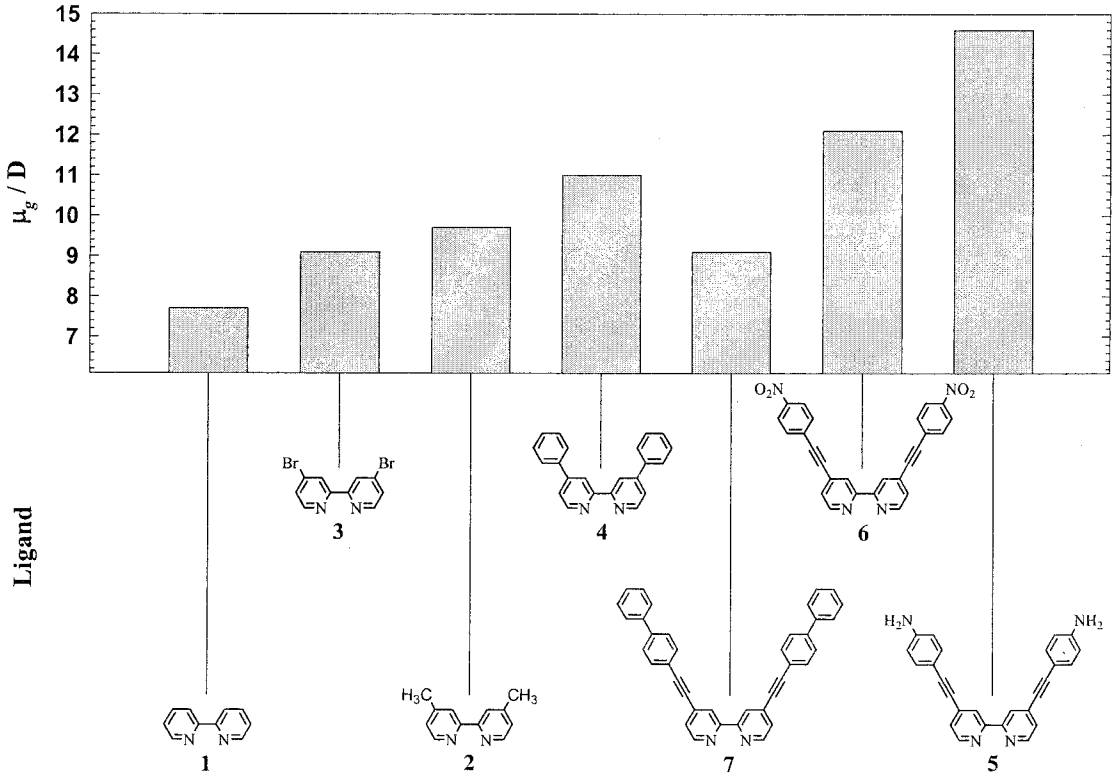

Figure 4. Experimentally determined ground-state dipole moments ($\mu_{g,exp}$) for (X_2-bpy)$Re^I(CO)_3Cl$ complexes **1**−**7**.

rhenium, calculations were performed on manganese analogues of **1**−**7**. The calculated values ($\mu_{g,calcd}$) significantly exceed the experimental values. Nevertheless, with the exception of **7**, a fair correlation exists between $\mu_{g,calcd}$ (Mn) and $\mu_{g,exp}$ (Re). Advantage was taken of this correlation to extrapolate estimates for $\mu_{g,exp}$ (Re) for **5** and **6**, which are included in Table 3.

Returning to the calculations, the single most important structural factor in determining the relative magnitudes of $\mu_{g,calcd}$ within the series of tricarbonyl chloro compounds appeared to be the size of the diimine ligand rather than the electron-withdrawing or -donating strength of its substituents (see Figure 4). In other words, the total number of valence electrons within the ligand and its substituents appears to be more important than the electronegativities of the atoms comprising the substituents, at least for the limited range of substituents examined.

With estimates or measurements of μ_g in hand, values for the excited-state dipole moment and the scalar difference in dipole moment ($\Delta\mu_s$) can be obtained from the available TDCP parameters. These results are listed in Table 3. From the table, it is clear that electron-donating substituents render $\Delta\mu_s$ more negative, while the weak electron-withdrawing substituents in compound **3** lead to a slightly more positive value. Note that these substituents exert the opposite effect, in terms of absolute magnitude, to those observed for vector dipole moment changes, $|\Delta\mu_v|$. Aryl and ethynyl-aryl substituents exert a more substantial influence upon $\Delta\mu_s$, yielding less negative values than those recorded for the parent bipyridine compound **1** and other compounds lacking substituents capable of extending the ligand π system. Again, however, **7** deviates from the pattern.

The availability of both scalar (μ_g and μ_e) and vector ($|\Delta\mu_v|$) parameters permits the geometric relationship between ground- and excited-state dipole moments to be elucidated. The numerical inequivalence of the scalar and vector dipole moment changes is evidence for the noncollinearity of ground- and excited-state dipole moments. More quantitatively, the angle between μ_g and μ_e ($\theta_{\Delta\mu}$, the extent of rotation of the molecular dipole moment upon ^{3}MLCT excited-state formation) is given by the following expression:

$$|\Delta\mu_v|^2 = \mu_g^2 + \mu_e^2 - 2\mu_g\mu_e\cos(\theta_{\Delta\mu}) \qquad (12)$$

Values for $\theta_{\Delta\mu}$ based on eq 12 are listed in Table 3.[40] In all cases, the dipole moments deviate substantially from collinearity ($\theta_{\Delta\mu} = 0$). Notably, however, electron-withdrawing substitutents increase the dipole angle, while electron-donating substituents diminish it. Electron-delocalizing substituents (with the exception of **7**) also diminish the angle.

Discussion

(X_2-bpy)$Re^I(CO)_3Cl$ Energetics. Meyer and co-workers investigated the photophysical properties of a large series of (4,4′-X_2-bipyridine)$Re^I(CO)_3Cl$ complexes and uncovered trends that are replicated in this study.[18] They noted that, as one would anticipate, electron-donating substituents increase the energy of the ligand-based LUMO orbital energy, while

(40) Equation 8 assumes that dipole moments in solution are identical to those in rigid, polymeric environments. The assumption is probably least reasonable for compounds **4** and **7**. These almost certainly feature different μ_e values in the two environments, because of the ability of pendant phenyl groups, in solution, but not in rigid environments, to rotate and achieve coplanarity with the coordinated bipyridine radical anion created by photoexcitation.

Table 4. (X$_2$-bpy)Re^I(CO)$_3$Cl $\mu_{g,calcd}$ Data[a]

	X	$\mu_{g,calcd}$[b]/ D	$\mu_{g,Cl-M-OC}$[c]/ D	$\mu_{g,M-Cl}$[d]/ D	$\mu_{g,M-bpy}$[e]/ D	$\theta_{\mu g-bpy}$[f]/°
1	bpy	11.7	11.2	14.5	3.3	107
2	Me	12.5	10.9	14.2	6.2	120
3	Br	11.9	11.3	13.1	3.8	109
4	ϕ	12.8	10.5	12.5	7.3	125
5	DAE	14.3	11.5	13.1	8.5	127
6	DNE	13.3	11.7	14.4	6.4	119
7	DPE	13.1	10.6	12.3	7.7	126

[a] All calculations performed on geometry-optimized structures using ZINDO-1 semiempirical parameters. [b] Ground-state dipole moment determined by semiempirical calculations. [c] Component of $\mu_{g,calcd}$ aligned with the Cl−M−OC axis. [d] Component of $\mu_{g,calcd}$ associated with the M−Cl bond. [e] Component of $\mu_{g,calcd}$ associated with the M−bpy plane. [f] Angle between $\mu_{g,calcd}$ and the M−bpy plane. Angles over 90° indicate the dipole is pointing away from the diimine ligand.

electron-withdrawing substituents have the opposite effect. The energy of the rhenium dπ (HOMO) orbital is largely unaffected by the ligand substituents. These effects account for the observed sensitivity of ^{1}MLCT absorption and ^{3}MLCT luminescence energies to substituent electron-donation and -withdrawal properties. Again following Meyer and coworkers,[18] as well as McCusker et al.,[41] the energy-lowering effects of aryl and aryl-ethynyl substituents are ascribed to intraligand electronic delocalization in the MLCT excited state (i.e., expansion of the "π* box" occupied by the transferred electron).

Ground-State Dipole Moments. Measured ($\mu_{g,exp}$) ground-state dipole moments significantly exceed calculated ($\mu_{g,calcd}$) dipole moments (see Table 3). Comparison of **1** and **8** indicates that a portion of the discrepancy is due to replacement of rhenium by manganese in the semiempirical calculations, although substantial discrepancies remain. The calculations do, however, appear to capture the trends in the experimental data and thus should prove instructive in understanding the experimental behavior. The calculations further indicate that polarization of the metal−chloro bond, which is approximately orthogonal to the plane of the coordinated diimine ligand, accounts for a significant fraction of the total ground-state dipole moment of each compound. This finding is summarized in Table 4, where calculated dipole moments have been separated into vector components: (a) aligned with the carbonyl−metal−chlorine axis ($\mu_{g,Cl-M-OC}$), (b) associated specifically with the metal−chloro bond ($\mu_{g,M-Cl}$),[42] and (c) aligned with the metal−diimine plane ($\mu_{g,M-bpy}$). Also included are calculated μ_g angles with respect to the metal−diimine plane ($\theta_{\mu g-bpy}$). These parameters qualitatively corroborate the experimental observation that μ_g increases as the diimine ligand size increases (Figure 4), while also corroborating the expected (secondary) influence of electron-withdrawing and electron-donating properties of the diimine ligand substituents.

Charge Transfer Distance. As noted previously, the vector dipole moment change can be equated with the adiabatic charge-transfer distance (R_{12}), where 1 D = 0.21 e·Å. Values for R_{12} are listed in Table 2. Consistent with several previous studies of coordination complexes, internal charge transfer distances are much shorter than geometric donor−acceptor separation distances.[2,3,13,43] For example, molecular modeling produces a distance from rhenium to the center of the phenyl-substituted bipyridine ligand of **4** of 5.2 Å, more than double the effective CT distance returned by the Stark measurement.

One consequence, again noted in previous studies, is that initial-state/final-state electronic coupling energies (H_{ab}), as calculated from MLCT oscillator strengths via the two-state Hush model (eq 14),[3,5] are larger than one would anticipate on the basis of geometric CT distances.[5,44] The values obtained range from ~4000 cm^{-1} for **1** to ~7000 cm^{-1} for **7**, with significant uncertainty attending the estimates because of overlap of ^{1}MLCT transitions with other features in the electronic absorption spectrum. The availability of the coupling parameters permits diabatic charge transfer distances, R_{ab}, to be calculated from the adiabatic distances:[44,45]

$$\mathbf{P}_{12} = 2.06 \times 10^{-2}\left[\frac{\epsilon_{max}\Delta\upsilon_{1/2}}{\upsilon_{max}b}\right]^{1/2} \quad (13)$$

$$H_{ab} = \frac{\mathbf{P}_{12}\upsilon_{max}}{R_{12}e} \quad (14)$$

$$R_{ab} = \frac{R_{12}}{1 - 2(H_{ab}^2/\upsilon_{max}^2)} \quad (15)$$

In these equations, $\mathbf{P}_{12}$ is the transition dipole moment (closely related to the oscillator strength), υ_{max} is the band maximum, ϵ_{max} is the molar absorptivity at υ_{max}, $\Delta\upsilon_{1/2}$ is the absorption bandwidth, and b is the degeneracy term (2 in this case). We find in these complexes that the calculated diabatic distances are marginally greater, ~0.2 Å, than the measured adiabatic distances. Following Cave and Newton,[5] this difference can be interpreted as the amount that partial metal charge delocalization onto the ligand in the ground state, as well as ligand delocalization onto the metal in the excited state, contributes to the diminution of the effective CT distance. Clearly, the effect is small.[46] It seems likely that the balance of this effect comes from MLCT excited-state self-polarization and related phenomena (i.e., Re(II)/coordinated diimine radical anion Coulombic interactions).[14]

For the available compounds, the effective CT distance (or equivalently, $|\Delta\mu_v|$) increases with the addition of electron-withdrawing groups and decreases when electron-donating groups are incorporated. Substituent electronic

(41) Damrauer, N. H.; Boussie, T. R.; Devenney, M.; McCusker, J. K. *J. Am. Chem. Soc.* **1997**, *119*, 8253−8268.

(42) $\mu_{g,M-Cl}$ was calculated by multiplying the difference in charges on the two atoms by their separation distance.

(43) (a) Karki, L.; Lu, H. P.; Hupp, J. T. *J. Phys. Chem.* **1996**, *100*, 15637−15639. (b) Karki, L.; Hupp, J. T. *J. Am. Chem. Soc.* **1997**, *119*, 4070−4073.

(44) Creutz, C.; Newton, M. D.; Sutin, N. *J. Photochem. Photobiol. A* **1994**, *82*, 47−59.

(45) Vance, F. W.; Slone, R. V.; Stern, C. L.; Hupp, J. T. *Chem. Phys.* **2000**, *253*, 313−322.

(46) The effect may be even smaller than indicated because H_{ab} describes ground-state mixing with the initially formed and predominantly singlet MLCT excited state. Mixing with the predominantly triplet, emissive MLCT state presumably is less, making H_{ab} smaller and reducing the difference between R_{ab} and R_{12}.

properties necessarily influence both ground and excited states. The effects are greater, however, in the MLCT excited state. The differential effect is manifest as a change in $|\Delta\mu_v|$.

The effects of adding potentially electron-delocalizing groups are more complex. For example, the added phenyl rings of **4** do not dramatically increase the CT distance as measured by Stark emission spectroscopy, presumably because they lack coplanarity with the bipyridine portion of the ligand, thus limiting delocalization of the transferred charge. Indeed, McCusker and co-workers[41] showed that the phenyl rings in $Ru(d\phi\text{-bpy})_3^{2+}$ are canted between 40° and 50° with respect to the bipyridyl plane in the ground state. While the phenyl groups of **4** likely rotate to a coplanar conformation in the excited state in liquid environments,[41,47] the combination of low temperature (77 K) and immobilization of the sample in a polymer matrix precludes this motion under the conditions of the Stark experiment. This restriction reduces the ability of the rings to increase $|\Delta\mu_v|$. Further excited-state electronic delocalization likely occurs within the even larger ligand associated with complex **7**. Consistent with that reasoning, a still larger $|\Delta\mu_v|$ value is observed. However, the value is perhaps not as large as expected, presumably because of the second set of phenyl rings being partially orthogonal to the remainder of the ligand.

Scalar Dipole Moment Changes. As noted previously, $\Delta\mu_s$ values measured by TDCP seemingly respond in opposite fashion to $|\Delta\mu_v|$ when electron-withdrawing or electron-donating substituents are introduced. These apparently contradictory observations are actually self-consistent. Briefly, μ_g exceeds μ_e when scalar quantities are considered because of the large ground-state polarization of the Re−Cl bond. The addition of electron-withdrawing substituents will preferentially increase μ_e, leading to a smaller absolute scalar difference between μ_e and μ_g. While the difference between **1** and **3** is essentially equivalent to the experimental error, the proposed electron-withdrawing effect can more easily be observed when **4** and **6** are compared. The opposite effect occurs with electron-donating substituents, as observed in compounds **1** and **2**. When vector differences are considered, the greater influence of electron-donating (or -withdrawing) substituents upon the excited-state dipole moment decreases (or increases, respectively) the vector difference. The absolute value of this difference is the quantity measured by the Stark emission measurement.

Polarizability Changes. The observed large polarizability changes, and especially the differences in the $\Delta\alpha$ parameter sign for **1**−**4** versus **5**−**7**, are difficult to interpret in any detail. Brunschwig and co-workers, in their Stark absorption studies of ruthenium ammine complexes,[3,13,14] noted that a basic two-level electronic treatment yields an excited-state polarizability that is equal, but opposite in sign, to the necessarily positive polarizability of the ground state, making $\Delta\alpha_{e-g}$ a negative quantity. However, as additional excited states are incorporated, $\Delta\alpha_{e-g}$ is expected to become positive. The signs of $\Delta\alpha$ parameters have sometimes been interpreted as qualitative indicators of the relative importance of configuration interactions.

The measurements presented here involve transitions from the lowest electronic excited state to the ground state. Consequently, if sign conventions are preserved, polarizability changes measured by electroemission ($\Delta\alpha_{g-e}$) should be opposite in sign to those measured by electroabsorption ($\Delta\alpha_{e-g}$). To verify this supposition, we examined the model compound 4-(dimethylamino)-4′-nitrostilbene and obtained oppositely signed $\Delta\alpha$ parameters from the two techniques. Returning to the polarizability changes for the rhenium coordination complexes, one interpretation is that compounds **1**−**4** feature emissive MLCT excited states that are comparatively poorly mixed with upper excited states, while **5**−**7** feature emissive MLCT excited states that are more extensively mixed. Another interpretation emphasizes a more intuitive description: An excess electron in the extended π system of a large ligand, such as those found in MLCT excited states of **5**−**7**, will be comparatively easy to polarize. An electron confined to a d orbital on a single atom (Re) in the electronic ground state should be much less polarizable. The polarizability change upon excited-state to ground-state conversion should therefore be negative, consistent with experiment. The argument becomes less compelling as the size of the chromophoric ligand decreases (compounds **1**−**4**), and less negative, or even positive, polarizability changes are expected.

Dipole Moment Positioning. All of the TDCP signals obtained from the rhenium complexes are negative, indicating that μ_e is smaller in absolute magnitude than μ_g. Indeed, experiments as well as ZINDO-1 calculations here and in previous work[8] confirm that μ_g is relatively large ($\geq$8 D) and support the idea that $\mu_e < \mu_g$ even though an electron is promoted from the central metal to the bipyridine ligand. This dipole moment reduction upon excited-state formation provides an attractive explanation for the negative solvatochromism typically observed in these complexes.[15,17,18] Previously, this behavior has been ascribed to an unusually strong influence of solvent polarity on the internal molecular structure.[17]

A remaining question is why μ_e is smaller than μ_g, even in complexes with large, delocalized bipyridine ligands. The answer lies in the orientations of the individual dipole moments. Illustrations of the dipole positioning obtained from semiemiprical calculations and experimental results for complexes **1**, **3**, and **4** are shown in Scheme 3, where N⌒N represents the substituted bipyridine ligand. Note that these dipole moments extend to the center of mass in the molecule, which is located between the rhenium center and the bipyridine ligand and varies with bipyridine substitutent composition.[48] The ground-state dipole moment is largely oriented in the direction of the Re−Cl bond because of its

(47) (a) Schoonover, J. R.; Chen, P.; Bates, W. D.; Dyer, R. B.; Meyer, T. J. *Inorg. Chem.* **1994**, *33*, 793−797. (b) Chen, P.; Palmer, R. A.; Meyer, T. J. *J. Phys. Chem. A* **1998**, *102*, 3042−3047.

(48) The illustration of the dipole moments extending to the center of mass is a formalism of the Hyperchem calculation, but the calculated components of μ_g associated with the varying molecular axes are correct regardless of the spatial representation of the dipole moment.

Scheme 3

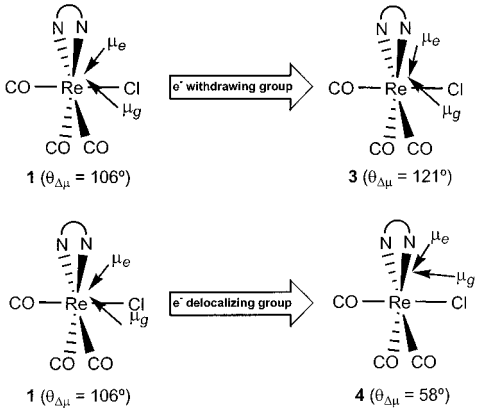

polarization but is partially rotated from collinearity with this bond because of the mass and electron density of the bipyridine ligand. Upon MLCT excitation, the dipole swings above the Re−Cl bond and closer to the bipyridine ligand where the photoexcited electron lies (see Scheme 3 for orientation). However, the resulting excited-state dipole moment is the sum of polarizations resulting from both electron promotion and residual Re−Cl bond polarization. It is this sum of these two differing, noncollinear contributions that leads to μ_e being smaller than μ_g.

Examination of the ligand-composition dependence of $\theta_{\Delta\mu}$ (Table 3) provides further insight into photoinduced dipole moment reorientation within these complexes. When an electron-withdrawing substituent is present on the bipyridine ligand (**3**), the excited-state dipole experiences more of a "pull" from the bipyridine, so it rotates closer to the plane of the bipyridine ligand. Furthermore, on the basis of calculations, μ_g remains essentially in the same orientation with respect to the Re−Cl bond (see Table 4), leading to a $\theta_{\Delta\mu}$ increase (Scheme 3). An electron-donating substituent exhibits the opposite effect in the sense that its "pull" on the dipole is decreased.

Introduction of electron-delocalizing substituents (**4**) causes a sharp decrease in $\theta_{\Delta\mu}$. This decrease stems from the dramatic "pull" exhibited on both μ_g and μ_e by the significantly more delocalizing diimine ligand coupled with a center of mass shift toward the ligand. Calculations further show that μ_g is influenced more than μ_e by this substitution, leading to the observed angle decrease. The substitution of electron-donating and -withdrawing substituents on the phenyl rings yields the same (qualitative) angle decreases and increases, respectively, for reasons analogous to those described previously. In contrast to other arene-substituted diimine complexes, **7** exhibits a large $\theta_{\Delta\mu}$ increase. One possible explanation is that the significant electron-withdrawing nature of ethynyl-biphenyl substitutents[12,49] more than offsets the $\theta_{\Delta\mu}$ attenuation expected from enhanced excited-state delocalization.

Conclusions

A series of (X$_2$-bipyridine)Re^I(CO)$_3$Cl complexes, where X is an electron-donating, -withdrawing, or -delocalizing substituent, have been synthesized, and their photophysical properties, including charge transfer properties, have been evaluated. A complementary pair of techniques, Stark emission spectroscopy and TDCP, provide information on both CT distances (vector dipole moment changes) and more general charge redistribution effects concomitant with MLCT excitation. Electron-donating substituents increase the MLCT transition energy and decrease the effective electron transfer distance, while electron-withdrawing and -delocalizing groups produce the opposite effect. The noncollinearity of the ground- and excited-state dipole moments presents an interesting opportunity to understand in a more detailed way the mechanics of charge transfer and redistribution in these complexes through determination of the angle between μ_g and μ_e. The angle is finite in all cases, indicating rotation of the dipole moment upon ^{3}MLCT state formation. Occurrence of nonzero angles is indicated by experimentally different absolute values for vector dipole moment changes (Stark emission measurements) versus scalar dipole moment changes (TDCP measurements). The angle between μ_g and μ_e is larger for complexes featuring electron-withdrawing groups than for complexes featuring either electron-donating groups or electron-delocalizing groups. These low symmetry compounds are additionally characterized by noncollinearity of the transition dipole moment and $\Delta\mu$ vectors.

Acknowledgment. We thank Dr. Frederik W. M. Vanhelmont for initial TDCP instrument implementation and preliminary measurements, Prof. Sergei Smirnov (New Mexico State University) and Prof. Linda Peteanu (Carnegie Mellon University) for helpful discussions, Prof. Frederick D. Lewis for the use of the luminescence lifetime instrument, Dr. Rajdeep Kalgutkar for his help with the luminescence lifetime measurements, and Dennis A. Gaal for the transient absorption lifetime measurements. We gratefully acknowledge financial support from the U.S. Department of Energy, Office of Science (Grant DE-FG02-87ER13808).

IC011015G

(49) (a) Ley, K. D.; Schanze, K. S. *Coord. Chem. Rev.* **1998**, *171*, 287−307. (b) Walters, K. A.; Ley, K. D.; Cavalaheiro, C. S. P.; Miller, S. E.; Gosztola, D.; Wasielewski, M. R.; Bussandri, A. P.; Van Willigen, H.; Schanze, K. S. *J. Am. Chem. Soc.* **2001**, *123*, 8329−8342.